Hindawi Publishing Corporation
Journal of Materials
Volume 2014, Article ID 318262, 8 pages
http://dx.doi.org/10.1155/2014/318262

Research Article

Effect of Sn Addition on Thermal and Optical Properties of $Pb_9Se_{71}Ge_{20-x}Sn_x$ $(8 \leq x \leq 12)$ Glass

Vivek Modgil and V. S. Rangra

Department of Physics, Himachal Pradesh University, Summerhill, Shimla 171005, India

Correspondence should be addressed to Vivek Modgil; vivekmodgilphysics.hpu@gmail.com

Received 10 November 2013; Revised 23 February 2014; Accepted 24 February 2014; Published 27 March 2014

Academic Editor: Te-Hua Fang

Study of thermal and optical parameters of $Pb_9Se_{71}Ge_{20-x}Sn_x$ $(8 \leq x \leq 12)$ glass has been undertaken. Crystallization and glass transition kinetics has been investigated under nonisothermal conditions by DSC technique. Phase separation has been observed in the material and is investigated by taking the XRD of annealed bulk samples. The material possesses good glass forming ability, high value of glass transition temperature about 420 K, and glass stability. Optical band gap and other optical constants such as refractive index and extinction coefficient have been determined. The isoelectronic substitution of Ge with Sn in the glassy system reduces the optical band gap and enhances the thermal properties.

1. Introduction

In amorphous semiconductors, among inorganic glassy materials, chalcogenide glasses occupy a unique place in material science towards advancement of technology. Generally these materials are weakly bonded materials than oxide glasses. But in comparison with amorphous silicon, halide glasses, and other group IV tetrahedral bonded semiconductors these materials exhibit the superior properties which can be tailored by varying the composition. The physical properties such as optical band gap, dielectric behavior, and conductivity of chalcogenide glasses mark their strong dependency on lone pair electrons and density of defect states in the band tails [1, 2]. The disorder in amorphous semiconductors causes perturbation in density of state functions resulting in band tails at the edges of the bottom of the conduction band and the top of the valence band [3]. The lone pair orbits have higher energy than the bonding states and hence occupy the top of the valence band. Interactions between lone pair electrons with their local environment and different atoms result in localized states in the band tails [4]. These localized states play crucial role in deciding optical properties of the materials.

The better optical and thermal properties of these materials make them of potential use in the technological applications such as in photonics and phase change memories because of higher values of refractive index and lower value of phonon energy of these glasses [5, 6]. The present Investigation on phase change memories (PCM) shows the possibility of obtaining multistate behavior, enhanced ability to withstand thermal cycling, and use of lower voltages for achieving desired phase change response by using the bilayers of Ge-chalcogenide and Sn-chalcogenide [7].

Germanium is a good glass former and has good glass forming region with Se but has the disadvantage that the Ge compositions have the wide optical band gap which results in the intrinsic optical loss and causes problem in long distance fiber communication. In order to remove such discrepancies chalcogen elements are added with heavy elements. Many researchers have carried out their work on this type of compositions such as Ge-Sb-Se, Ge-Sn-Se [8, 9], and Ge-Sn-Sb-Se [10] to improve the optical properties. These materials can be used in the photonic crystal applications due to their higher value of refractive index. Photonic crystals are the materials which are used in photonic applications, such as optical band gap devices and omnidirectional reflectors [6].

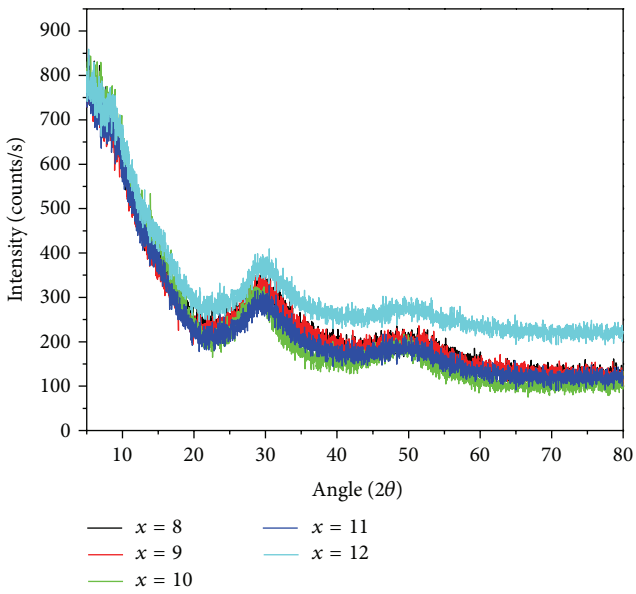

FIGURE 1: X-ray diffractograms of the chalcogenide glass $Pb_9Se_{71}Ge_{20-x}Sn_x$ ($8 \le x \le 12$).

It is necessary to have the knowledge of thermal stability and glass-forming ability (GFA) of material to know its suitability for the particular technological application before crystallization takes place. The addition of elemental impurity such as Ge, Sn, In, and Pb has a pronounced effect on structural, optical, electronic, and thermal properties of material [11–15]. The addition of Sn may expand and create compositional and configurational disorder in material and accordingly modifies the properties. The Sn has been added in Pb-Se-Ge system to see the effect of Sn incorporation on thermal and optical behaviors of this material.

2. Experimental Details

2.1. Material Synthesis and Characterization. The chalcogenide materials $Pb_9Se_{71}Ge_{20-x}Sn_x$ ($8 \le x \le 12$ at.%) are prepared by the melt quenching technique. Granules of Pb and powder of Sn, Ge, and Se having 99.999% purity are used. The material is then sealed in evacuated (~10^{-5} Torr) quartz ampoule (length ~15 cm and internal diameter ~8 mm). The ampoules containing material are heated to 1000°C and held at that temperature for 10 hours. The temperature of the furnace is raised slowly at a rate of 3-4°C per minute. During heating, the ampoule is constantly rocked. The obtained melt is quenched in ice cool water. The nature of the material is ascertained by powder X-ray diffraction technique. For this, X-ray diffraction (XRD) patterns of sample are taken at room temperature by using an X-ray diffractometer PANalytical X'pert Pro (PW 3050/60, $CuK_{\alpha 1}$ $\lambda = 1.54$ Å) shown in Figure 1.

The thermal behavior of the material has been studied using differential scanning calorimetry (DSC) under nonisothermal conditions using DSC instrument Mettler Star SW 9.01 model. Approximately 15–20 mg quantity of each powdered sample is used for DSC analysis. Each sample is heated at different heating rates 10, 15, 20, and 25°k/minute. We have found that material's samples at $x = 11, 12$ have double crystallization peaks which are due to the phase separation in the material. We have annealed the bulk sample $x = 11$ at temperatures 507 K and 550 K for 3 hours to detect the phases separated in the material. Then XRDs of samples have been taken. Figure 4 shows the XRD patterns of the annealed samples ($x = 11$). To find out the band gap and other optical constants, thin films of chalcogenide glasses have been deposited by vacuum evaporation technique on thoroughly cleaned microscope glass substrate. The room-temperature optical transmission and absorption spectra (not shown here) at normal incidence, of the samples, are recorded over the 200 nm to 2500 nm spectral region, by a double-beam UV/Vis/NIR spectrophotometer (Perkin-Elmer, model Lambda-750).

3. Results and Discussions

3.1. Structural and Thermal Analysis. XRD diffractograms of the $Pb_9Se_{71}Ge_{20-x}Sn_x$ ($x = 8, 9, 10, 11, 12$ at.%) compositions are shown in Figure 1 which confirm the amorphous nature of material. In the diffractograms of glasses there are two types of halos, one big halo in 2θ range 25°–35°, confirming the polymeric nature and the short range order of the material and appearing predominately in all the diffractograms. The second small halo is between 45° and 55°; this halo appears slightly at $x = 10$ but appears significantly for samples $x = 11, 12$. That is because of partial phase separation in the material caused due to increasing concentration of Sn in the material.

When the material is heated under nonisothermal conditions at constant heating rate in DSC experiment, glass undergoes the structural variations and crystallizes. The variation of glass transition temperature, crystallization temperature, with varying Sn concentration can be studied by comparing the DSC thermograms of all samples at the same heating rate. Figure 2 shows the DSC thermograms of $Pb_9Se_{71}Ge_{20-x}Sn_x$ ($8 \le x \le 12$ at.%) material at a heating rate of 10 K min^{-1}. To know the thermodynamics of the material such as phase transformation, activation energy of glass transition, and crystallization, each sample is heated at four different heating rates. Figure 3 shows the DSC thermograms of $x = 12$ at different heating rates. Similar variation in the thermograms of other samples has been observed at different heating rates.

The glass up to atomic percentage $x = 10$ of Sn shows the single crystallization peak and at $x = 11, 12$ shows the double crystallization peaks. This appearance of double crystallization is because of partial phase separation in material. Phase separation is the unmixing of the initially homogeneous multicomponent material in to two or more amorphous phases. The driving potential for unmixing process is the reduction in the system free energy. Phase separation occurs when the free energy of another phase or polyphase is less than that of initially homogeneous single phase composition. In order to identify the phases in material, the initial glassy sample

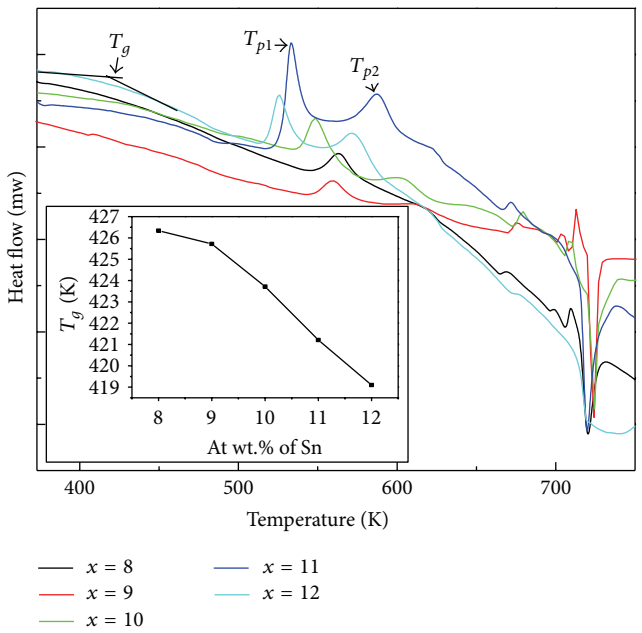

FIGURE 2: DSC thermograms of the samples at heating rate of 10 K/min.

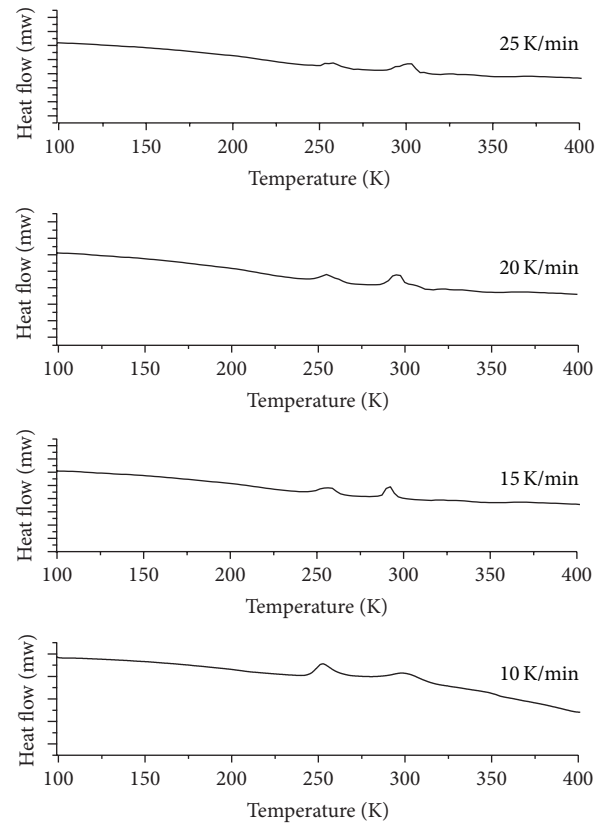

FIGURE 3: DSC thermograms of $Pb_9Se_{71}Ge_8Sn_{12}$ at different heating rate.

$Pb_9Se_{71}Ge_9Sn_{11}$ is annealed at 507 K and 550 K for 3hours, which lies before the primary and secondary crystallization, respectively. The annealed samples are then passed through XRD.

Figure 4 shows the XRD patterns of the annealed samples. After annealing the samples for 3 hours, we have observed the two major phases $SnSe_2$ and $GeSe_2$ and minor phase PbSe as marked in XRD diffractograms. $GeSe_2$ has monoclinic structure and lattice parameters $a = 7.231$ Å, $b = 16.748$ Å, and $c = 11.79$ Å [JCPDS file card no. 30-0595]. The $SnSe_2$ structure is formed in such a way that Sn layer is sandwiched between the two Se layers facing towards each other. The $SnSe_2$ has the hexagonal structure having $a = 3.84$ Å, $b = 1.61$ Å, and $c = 6.18$ Å [JCPDS file card no. 38-1055] and Pb-Se phase has the cubic structure whose lattice parameter is $a = 6.089$ Å. When the sample is annealed at temperature 550 K, mainly $GeSe_2$ phase remains and other phases reduce to a large extent.

On the basis of chemical bond approach [16], with increase of Sn content, glass transition temperature decreases because Ge-Se bonds are replaced by the Sn-Se bonds. From Figure 4 it is clear that glass at $x = 11, 12$ has been phase separated into two main phases, one Ge-rich and the other Sn-rich. The higher and lower Tc may be due to Ge-rich and Sn-rich phase, respectively.

3.2. Kinetics of Phase Transformations

3.2.1. Glass Transition Region. The variations of glass transition temperature, activation energy of glass transition (E_g) with composition have been studied. The dependence of T_g on heating rate (α) is hereby discussed on the basis of two approaches. The first approach is the empirical relation suggested by Lasocka [17]:

$$T_g = A + B \ln \alpha, \tag{1}$$

where A and B are constants for a given glass composition. The value of A indicates the glass transition temperature for the heating rate of 1 K min^{-1}, while the value of B determines the time response of configurational changes within the glass transition region to the heating rate, shown in Table 1. This equation is found to hold well for all samples. Figure 5 depicts the plots of T_g versus $\ln(\alpha)$ for the investigated $Pb_9Se_{71}Ge_{20-x}Sn_x$ glassy system.

The second approach Kissinger equation shows the dependence of T_g on heating rate [18, 19]. This equation is

TABLE 1: The values of glass transition temperature, A and B constants from Lasocka formulation, and activation energy of samples by Kissinger and Moynihan approach.

x	T_g	Lasocka approach		Kissinger	Moynihan
		A	B (min)	E_g (kJ/mol)	E_g (kJ/mol)
8	426.34	412.920	5.700	254.062	261.183
9	425.72	413.505	4.918	224.536	231.656
10	423.72	413.840	4.212	338.300	345.364
11	421.21	411.550	4.034	314.118	321.182
12	419.10	407.556	4.918	285.947	293.011

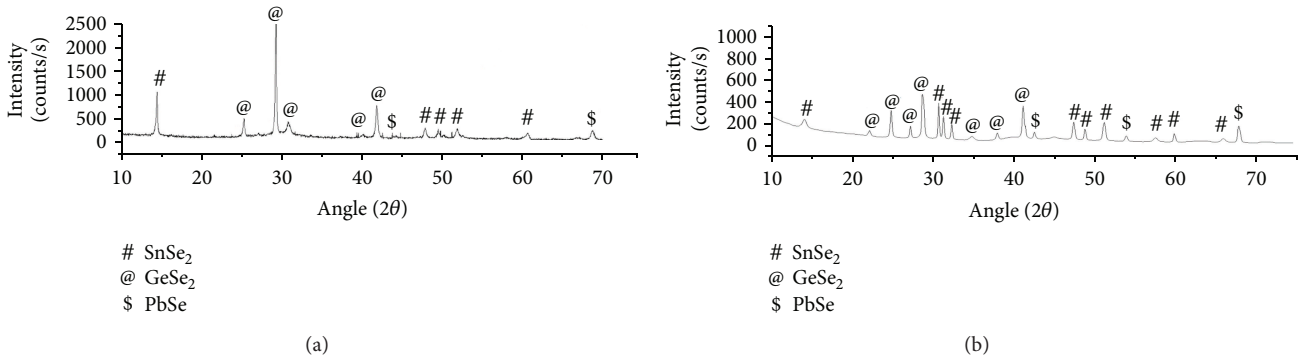

FIGURE 4: X-ray diffractograms of sample $Pb_9Se_{71}Ge_9Sn_{11}$ annealed at (a) 550 K and (b) 507 K.

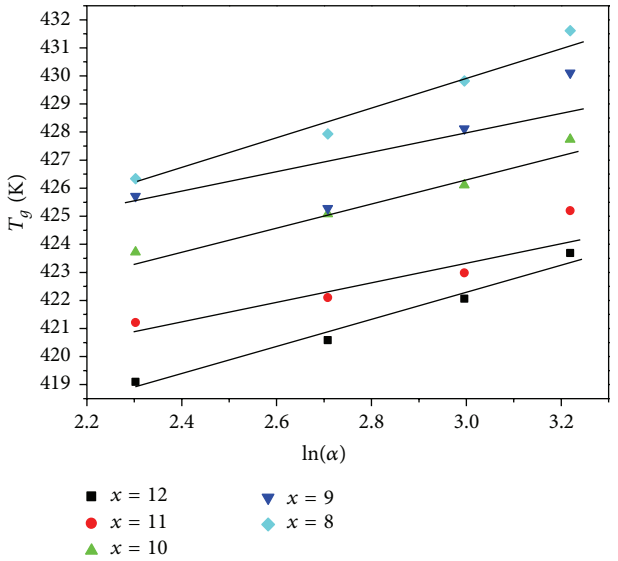

FIGURE 5: Plot of $\ln \alpha$ against T_g.

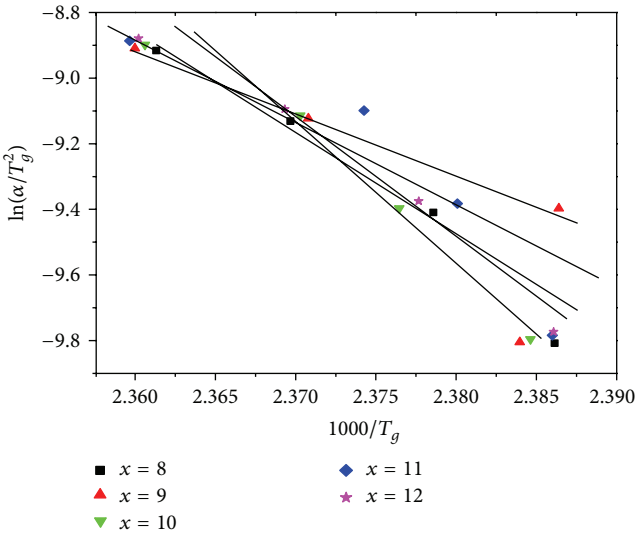

FIGURE 6: Plot between $\ln(\alpha/T_g^2)$ and $1000/T_g$ from Kissinger equation.

used to find out the activation energy of glass transition. Kissinger equation is basically used to find activation energy of crystallization process; it can also be used for the determination of the activation energy of glass transition using the peak glass transition temperatures under nonisothermal conditions, if similar shift observed in the glass transition peaks and crystallization peaks with heating rate. As thermal mechanism varies with temperature, the position of peaks also varies with the heating rate. This temperature shift, in turn, can be used for the determination of kinetic parameters of crystallization [20]. Hence Kissinger equation relating the peak glass transition temperature and heating rate is given by

$$\ln\left(\frac{\alpha}{T_g^2}\right) = \frac{-E_g}{RT_g} + \text{constant}, \tag{2}$$

where T_g is the peak glass transition temperature and R is the gas constant.

A graph is plotted between $\ln(\alpha/T_g^2)$ and $1000/T_g$ shown in Figure 6, which yields a straight line. The slope $(-E_g/R)$ of the straight line gives the activation energy of glass transition. The one more approach used for calculation of activation energy of glass transition is Moynihan's relation [21] Moynihan has found in his derivation of the dependence of T_g on heating rate $|\alpha|$. Accordingly for a given heating rate

$$\frac{d\ln|\alpha|}{d\left(1/T_g\right)} \approx \frac{-E_g}{R}. \tag{3}$$

Plots of $\ln \alpha$ against $1000/T_g$ are plotted for various glassy alloys shown in Figure 7. The values of activation energies found by Kissinger and Moynihan approaches are tabulated in Table 2.

Activation energy of glass transition decreases as x varies from 8 to 9. This is due to entrance of Sn in Pb-Se-Ge network, which weakens the network and decrease the activation energy of glass transition. Thenafter at $x = 10$ this activation energy increases which might be due to replacement of Se-Se bonds by Sn-Se bonds (having large bond energy). The further addition of Sn to the glass matrix replaces mostly

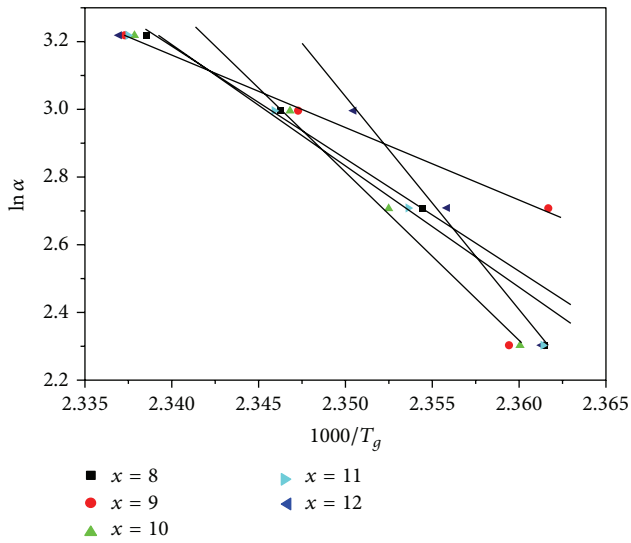

Figure 7: Plots of ln α against $1000/T_g$ glassy alloys from Moynihan equation.

Table 2: The values of activation energies of crystallization calculated by Kissinger and Augis and Bennett approaches.

x	Activation energies of crystallization (KJ/mol)			
	Kissinger		Augis and Bennett	
	Peak 1	Peak 2	Peak 1	Peak 2
8	205.074		209.794	
9	249.723		254.394	
10	118.924		126.432	
11	204.919	313.630	211.39	324.525
12	173.512	189.093	178.315	196.375

the Ge-Se bonds by Sn-Se bonds. So it results in decrease in cohesive energy and mean bond energy of the glassy matrix as well as the activation energy of glass transition.

3.2.2. Activation Energy of Crystallization. For the determination of crystallization kinetics, the established Kissinger and Augis-Bennett models are applied.

(a) Kissinger Model. The activation energy for crystallization, E_c, can be obtained from the dependence of peak crystallization temperature T_p on heating rate, using the equation derived by Kissinger [18, 19]:

$$\ln\left(\frac{\alpha}{T_p^2}\right) = \frac{-E_c}{RT_p} + \text{constant}. \quad (4)$$

The plot of $\ln(\alpha/T_p^2)$ versus $1000/T_p$ is shown in Figure 8. The activation energy of crystallization is calculated from slope of the straight lines in Figure 8 and tabulated in Table 3.

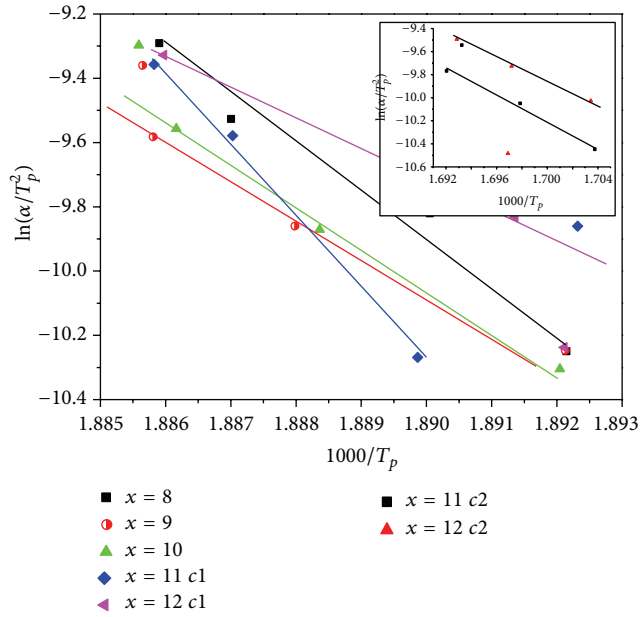

Figure 8: The plot of $\ln(\alpha/T_p^2)$ versus $1000/T_p$ for Kissinger approach.

Table 3: Values of refractive index (n), extinction coefficient (k), optical energy gap (E_g^{opt}), and real part (ε_r) and imaginary part (ε_i) of dielectric constant.

x	n	k	E_g^{opt}(eV)	ε_i	ε_r
8	2.21	0.0185	2.76	0.0817	4.8837
9	2.94	0.0219	2.71	0.1287	8.6431
10	3.19	0.0384	2.62	0.2449	10.1746
11	3.58	0.0515	2.56	0.3687	12.8137
12	3.71	0.0606	2.48	0.4496	13.7604

(b) Augis and Bennett Method. The activation energy for crystallization, E_c, can be evaluated using the formula suggested by Augis and Bennett [22] which is given as follows:

$$\ln\left(\frac{\alpha}{T_p}\right) = -\left(\frac{E_c}{RT_p}\right) + \text{constant}. \quad (5)$$

The plot of $\ln(\alpha/T_p)$ versus $1000/T_p$ is shown in Figure 9. The calculated activation energies of crystallization are tabulated in Table 3.

The addition of Sn causes the structural disorder in the glassy matrix; beyond $x = 10$ phase separation in the material has been found. Mainly two phases $GeSe_2$ and $SnSe_2$ appear in the material which causes phase splitting and double crystallization peaks. The peak at high crystallization temperature is due to $GeSe_2$ phase and at lower temperature due to $SnSe_2$ phase. We analyze from Table 2 that activation energies obtained from Augis and Bennett method is approximately around the activation energies obtained from the Kissinger's approach. However, this slight difference in the activation energies obtained by these approaches may be attributed to the different formalism of the equations in these models based on approximations. The addition of Sn has

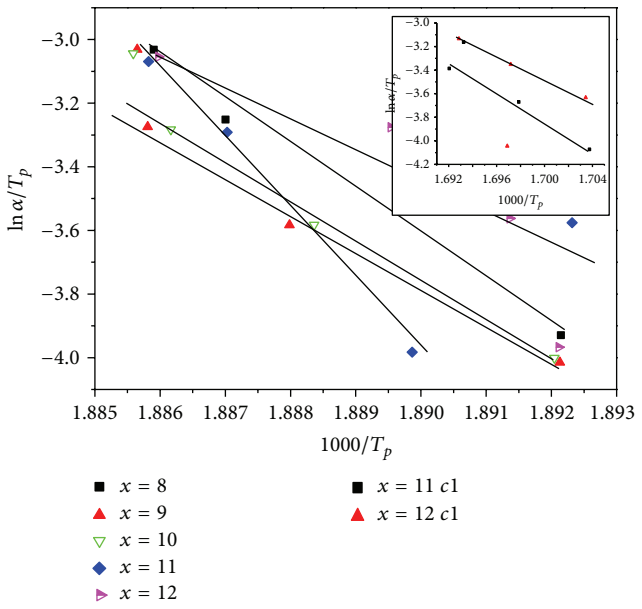

FIGURE 9: The plot of $\ln(\alpha/T_p)$ versus $1000/T_p$ for Augis and Bennett approach.

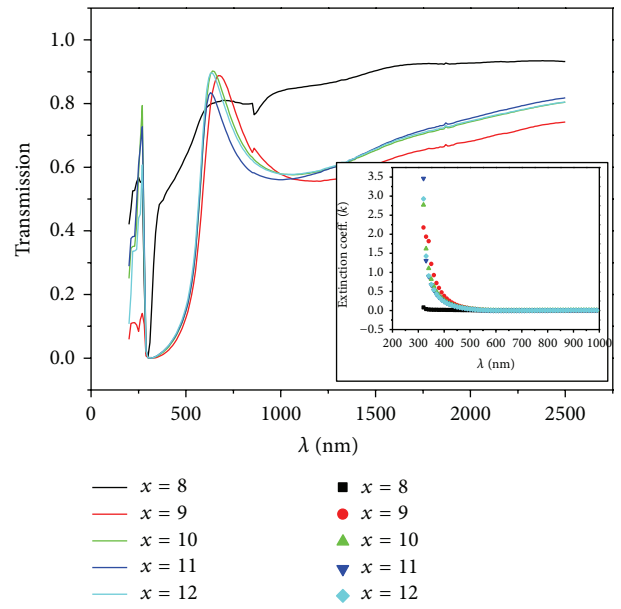

FIGURE 10: The transmission spectrum and variation of extinction coefficient with wavelength of chalcogenide glass thin films of $Pb_9Se_{71}Ge_{20-x}Sn_x$.

caused the structural disorder or configurational changes in the material. Beyond $x = 10$ phase separation in the material has been observed. The double crystallization peaks in the material are due to phase splitting into two amorphous phases $GeSe_2$ and $SnSe_2$. In double crystallization peaks, the high crystallization temperature peak is due to Ge-rich phase and peak at lower crystallization temperature is due to Sn-rich phase.

3.3. Optical and Dielectric Parameters. Generally the optical band gap and refractive index (n) are the basic parameters to know the material's optical behavior. The refractive index changes under the influence of light. The optical constants are calculated using Swanepoel's method. According to Swanepoel's method [23, 24], the value of the refractive index of film in the spectral region of medium and weak absorption can be calculated by the expression

$$n = \left[N + \left(N^2 - s^2\right)^{1/2}\right]^{1/2}, \tag{6}$$

where

$$N = 2s\frac{T_M - T_m}{T_M T_m} + \frac{s^2 + 1}{2}, \tag{7}$$

where T_M and T_m are the transmission maximum and the corresponding minimum at a certain wavelength λ. The transmission spectra of material are shown in Figure 10.

The spectra for $x = 8$ is different than that for others. This might be due to some foreign element introduction at the time of bulk or thin film preparation; this has created some compositional disorder in material. The value of extinction coefficient (k) has been calculated using the relation

$$k = \frac{\alpha\lambda}{4\pi}, \tag{8}$$

where α is the absorption coefficient [24] and is given by

$$\alpha = \frac{1}{d}\ln\left(\frac{1}{x}\right), \tag{9}$$

where x is the absorbance. The variations of the extinction coefficient with the wavelength are shown in Figure 10 inset.

The optical absorption spectrum is the important tool for studying the band gap of materials. The absorption coefficient of an amorphous semiconductor in the high absorption region can be calculated by using Tauc's relation [25] $\alpha h\nu = B(h\nu - E_g^{\text{opt}})^m$ where B is a constant, E_g^{opt} is the optical energy gap of the material, and m determines the type of transition ($m = 1/2$ for the direct transition and $m = 2$ for the indirect allowed transition).

The values of the optical energy gap (E_g^{opt}) obtained for indirect allowed transition for thin films of $Pb_9Se_{71}Ge_{20-x}Sn_x$ by making $(\alpha h\nu)^{0.5} \rightarrow 0$ are given in Table 3 and shown in Figure 11. The optical parameters refractive index (n) and extinction coefficient k have the compositional dependence as both increase with increasing Sn content. In covalent solids, variation in charge density results change in bond polarizability and hence permittivity; this variation alters the refractive index and the extinction coefficient of the material [26]. Optical constants (n, k) in anisotropic media depend on electronic polarization of atoms, ions, or molecules of the material when subjected to an electric field. The polarization does not respond instantly to an applied field and results in

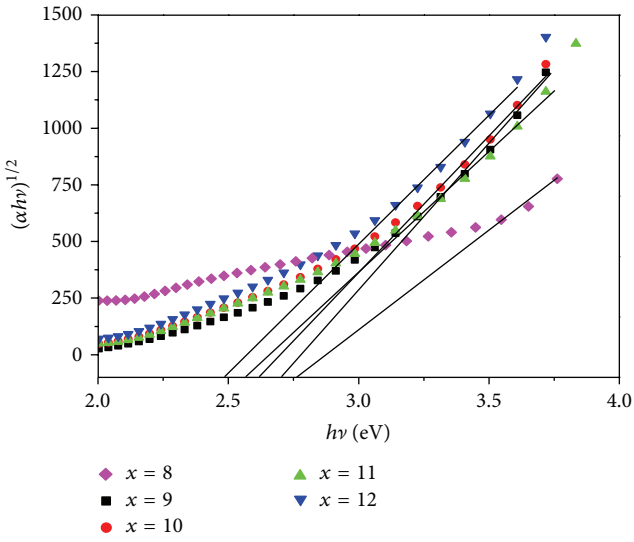

FIGURE 11: Plots of $(\alpha h\nu)^{0.5}$ versus $(h\nu)$ for thin films of $Pb_9Se_{71}Ge_{20-x}Sn_x$.

dielectric loss expressed as permittivity (ε), which is complex and frequency dependent and is given as $\varepsilon = \varepsilon_r + i\varepsilon_i$, where ($\varepsilon_r$) and ($\varepsilon_i$) are real and imaginary parts of permittivity, respectively. The complex dielectric constant is a fundamental intrinsic property of material. The real (ε_r) and imaginary (ε_i) parts of the dielectric constant of thin films were also calculated by using the value of n and k in the following relations [27]:

$$\varepsilon_r = n^2 - k^2, \tag{10}$$

$$\varepsilon_i = 2nk. \tag{11}$$

It is evident from Table 3 that the values of ε_r and ε_i increase on incorporating Sn into the Pb-Se-Ge system. Sn may cause the more defect states in the chalcogenide glasses. These defect states in turn can increase the density of localized states which reduces the optical band gap.

4. Conclusion

The thermal and optical properties of the Pb-Ge-Se system have been greatly influenced by Sn addition. The phase transformation kinetics of $Pb_9Se_{71}Ge_{20-x}Sn_x$ glasses has been studied using Kissinger, Moynihan, and Augis approaches. The glassy alloys under investigation (except $x = 11, 12$) show a single glass transition and crystallization region, confirming the homogeneity of the samples. Samples ($x = 11, 12$) show a single glass transition and double crystallization peaks corresponding to $SnSe_2$ and $GeSe_2$ rich phases. It is observed that glass transition temperature decreases with increasing Sn concentration. The glassy material has high value of refractive index and decreasing optical band gap with increasing content of Sn in the glassy matrix.

Conflict of Interests

The authors declare that there is no conflict of interests regarding the publication of this paper.

References

[1] S. R. Elliott, C. N. R. Rao, and J. M. Thomas, "The chemistry of the Noncrystalline State," *Angewandte Chemie International Edition*, vol. 25, pp. 31–46, 1986.

[2] R. M. Mehra, A. Ganjoo, and P. C. Mathur, "Electrical and optical properties of amorphous $(Se_{0.7}Te_{0.3})_{100-x}In_x$ system," *Journal of Applied Physics*, vol. 75, no. 11, pp. 7334–7339, 1994.

[3] N. F. Mott and E. A. Davis, *Electronic Process in Non-Crystalline Materials*, Clarendon, Oxford, UK, 1979.

[4] M. Kastner, D. Adler, and H. Fritzsche, "Valence-alternation model for localized gap states in lone-pair semiconductors," *Physical Review Letters*, vol. 37, no. 22, pp. 1504–1507, 1976.

[5] C. Meneghini and A. Villeneuve, "As_2S_3 photosensitivity by two-photon absorption: holographic gratings and self-written channel waveguides," *Journal of the Optical Society of America B: Optical Physics*, vol. 15, no. 12, pp. 2946–2950, 1998.

[6] K. Paivasaari, V. K. Tikhomirov, and J. Turunen, "High refractive index chalcogenide glass for photonic crystal applications," *Optics Express*, vol. 15, no. 5, pp. 2336–2340, 2007.

[7] A. Devasia, S. Kurinec, K. A. Campbell, and S. Raoux, "Influence of Sn Migration on phase transition in GeTe and Ge_2Se_3 thin films," *Applied Physics Letters*, vol. 96, no. 14, Article ID 141908, 2010.

[8] L. E. McNeil, J. M. Mikrut, and M. J. Peters, "Phase separation in $Ge_{1-x}Sn_xSe_2$ glasses," *Solid State Communications*, vol. 62, no. 2, pp. 101–103, 1987.

[9] J. M. Mikrut and L. E. McNeil, "Photostructural changes in bulk amorphous $Ge_{1-x}Sn_xSe_2$," *Journal of Non-Crystalline Solids*, vol. 114, no. 1, pp. 127–129, 1989.

[10] E. A. Kislitskaya and V. F. Kokorina, "Effect of the replacement of germanium by tin on glass formation and the physicochemical properties of glasses in the antimony-germanium-selenium system," *Zhurnal Prikladnoi Khimii*, vol. 44, pp. 646–648, 1971, Translated.

[11] M. M. Wakkad, E. Kh. Shokr, and Sh. Mohamed, "Crystallization kinetics and some physical properties of as-prepared and annealed Ge-Sb-Se chalcogenide glasses," *Physica Status Solidi A: Applications and Materials*, vol. 183, pp. 399–411, 2001.

[12] G. Mathew, K. N. Madhusudanan, and J. Philip, "Characteristics of photoconductivity in amorphous $Ge_xSb_{10}Se_{90-x}$ thin films," *Physica Status Solidi A: Applications and Materials*, vol. 168, pp. 239–248, 1998.

[13] N. B. Maharjan, K. Singh, and N. S. Saxena, "Calorimetric studies in $Se_{75}Te_{25-x}Sn_x$ chalcogenide glasses," *Physica Status Solidi A: Applications and Materials*, vol. 195, no. 2, pp. 305–310, 2003.

[14] G. Kaur and T. Komatsu, "Crystallization behavior of bulk amorphous Se-Sb-In system," *Journal of Materials Science*, vol. 36, no. 18, pp. 4531–4533, 2001.

[15] M. S. Kamboj and R. Thangaraj, "Calorimetric studies of bulk Se-Te-Pb glassy system," *The European Physical: Journal Applied Physics*, vol. 24, no. 1, pp. 33–36, 2003.

[16] J. Bicerano and S. R. Ovshinsky, "Chemical bond approach to the structures of chalcogenide glasses with reversible switching properties," *Journal of Non-Crystalline Solids*, vol. 74, no. 1, pp. 75–84, 1985.

[17] M. Lasocka, "The effect of scanning rate on glass transition temperature of splat-cooled $Te_{85}Ge_{15}$," *Materials Science and Engineering*, vol. 23, no. 2-3, pp. 173–177, 1976.

[18] H. E. Kissinger, "Variation of peak temperature with heating rate in differential thermal analysis," *Journal of Research of the National Bureau of Standards*, vol. 57, pp. 217–221, 1956.

[19] H. E. Kissinger, "Reaction kinetics in differential thermal analysis," *Analytical Chemistry*, vol. 29, no. 11, pp. 1702–1706, 1957.

[20] K. White, R. L. Crane, and J. A. Snide, "Crystallization kinetics of $As_{2-x}Sb_xS_3$ glass in bulk and thin film form," *Journal of Non-Crystalline Solids*, vol. 103, no. 2-3, pp. 210–220, 1988.

[21] C. T. Moynihan, A. J. Easteal, J. Wilder, and J. Tucker, "Dependence of the glass transition temperature on heating and cooling rate," *Journal of Physical Chemistry*, vol. 78, no. 26, pp. 2673–2677, 1974.

[22] J. A. Augis and J. E. Bennett, "Calculation of the Avrami parameters for heterogeneous solid state reactions using a modification of the Kissinger method," *Journal of Thermal Analysis*, vol. 13, no. 2, pp. 283–292, 1978.

[23] J. C. Manifacier, J. Gasiot, and J. P. Fillard, "A simple method for the determination of the optical constants n, k and the thickness of a weakly absorbing thin film," *Journal of Physics E: Scientific Instruments*, vol. 9, no. 11, pp. 1002–1004, 1976.

[24] R. Swanepoel, "Determination of the thickness and optical constants of amorphous silicon," *Journal of Physics E: Scientific Instruments*, vol. 16, no. 12, pp. 1214–1222, 1983.

[25] J. Tauc, *The Optical Properties of Solids*, pp. 171–180, North-Holland Publishing, Amsterdam, The Netherlands, 1970.

[26] A. Ganjoo and H. Jain, "Millisecond kinetics of photoinduced changes in the optical parameters of a-As_2S_3 films," *Physical Review B—Condensed Matter and Materials Physics*, vol. 74, no. 2, Article ID 024201, 11 pages, 2006.

[27] M. M. Wakkad, E. K. Shokr, and S. H. Mohamed, "Optical and calorimetric studies of Ge-Sb-Se glasses," *Journal of Non-Crystalline Solids*, vol. 265, no. 1, pp. 157–166, 2000.